analytical chemistry

Article

Cite This: Anal. Chem. 2019, 91, 3997−4003

pubs.acs.org/ac

Image-Based Investigation: Biorelevant Solubility of α and γ Indomethacin

Jernej Štukelj,*[,†,‡] Sami Svanbäck,[‡,†] Julijana Kristl,[§] Clare J. Strachan,[†] and Jouko Yliruusi[†]

[†]Division of Pharmaceutical Chemistry and Technology, University of Helsinki, Viikinkaari 5E, 00790 Helsinki, Finland

[‡]The Solubility Company, Viikinkaari 6, 00790 Helsinki, Finland

[§]University of Ljubljana, Faculty of Pharmacy, Aškerčeva 7, 1000 Ljubljana, Slovenia

Supporting Information

ABSTRACT: Solubility is a physicochemical property highly dependent on the solid-state form of a compound. Thus, alteration of a compound's solid-state form can be undertaken to enhance the solubility of poorly soluble drug compounds. In the Biopharmaceutics Classification System (BCS), drugs are classified on the basis of their aqueous solubility and permeability. However, aqueous solubility does not always correlate best with in vivo solubility and consequently bioavailability. Therefore, the use of biorelevant media is a more suitable approach for mimicking in vivo conditions. Here, assessed with a novel image-based single-particle-analysis (SPA) method, we report a constant ratio of solubility increase of 3.3 ± 0.5 between the α and γ solid-state forms of indomethacin in biorelevant media. The ratio was independent of pH, ionic strength, and surfactant concentration, which all change as the drug passes through the gastrointestinal tract. On the basis of the solubility ratio, a free-energy difference between the two polymorphic forms of 2.9 kJ/mol was estimated. Lastly, the use of the SPA approach to assess solubility has proven to be simple, fast, and both solvent- and sample-sparing, making it an attractive tool for drug development.

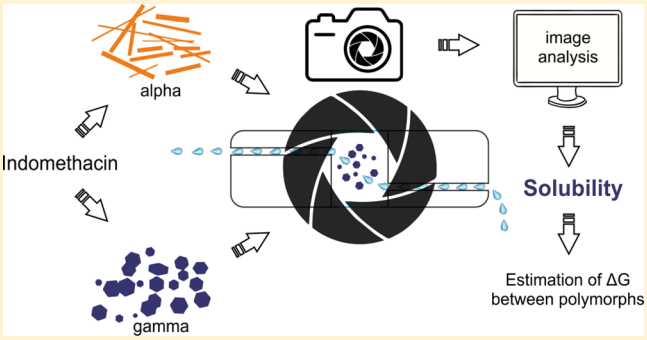

The effect of a drug in the body is a consequence of an intriguing interplay on the molecular level, with potency and selectivity being two values we use to characterize it. These two parameters, as crucial as they might seem, are not vital in determining the developability of a drug: stability and solubility are.[1−3] Furthermore, solubility is not only a molecular property; it is also highly governed by a compound's solid-state form.[2,4]

The rise of a new solid-state form in drug development can cause serious complications. Norvir is an illustrative example; two years after the product was launched, ritonavir, the active ingredient, transformed from Form I into a more thermodynamically stable Form II.[5] The new polymorph exhibited significantly reduced solubility resulting in lower bioavailability. Therefore, for a compound entering the development stage, it is wise to have a well-established polymorphic map with the corresponding thermodynamic relationships. Thermodynamic relationships are usually approached through the means of thermal analysis but can also be estimated from solubility data.[6,7] The obtained knowledge may thereafter be used for the deliberate alteration of a compound's solid-state form as an option to enhance its druglike properties (i.e., solubility).[8,9] This is especially true in these times of high-throughput screening (HTS) and combinatorial chemistry, when poor aqueous solubility is becoming a major issue in the drug-development process.[3,4]

In its most basic definition, thermodynamic-equilibrium solubility refers to the maximum amount of the most stable crystalline form of the compound that can remain dissolved in a given volume of the solvent at a given temperature and pressure.[8,10,11] The solubility of higher-energy solid-state forms (i.e., amorphous and metastable polymorphic forms) is referred to as "apparent solubility".[9,12] Therefore, starting the solubility measurement with a higher-energy solid-state form will initially produce the apparent solubility, but given enough time, the thermodynamic-equilibrium solubility of the most stable form will eventually dominate.

On the basis of aqueous solubility and permeability over a pH range of 1−7.5, drugs are categorized using the Biopharmaceutics Classification System (BCS).[13] Over the time the BCS has been in use, it has become apparent that further refinements are required, especially with regard to the in vivo correlation between dissolution and solubility.[14] Bergström et al. showed that the apparent BCS classification

Received: November 15, 2018
Accepted: February 20, 2019
Published: February 20, 2019

DOI: 10.1021/acs.analchem.8b05290
Anal. Chem. 2019, 91, 3997−4003

Table 1. Composition and Properties of Prepared Media[a]

	HCl	$FaSSGF_{blk}$	FaSSGF	$FeSSIF_{blk}$	FeSSIF
pH	1.6	1.6	1.6	5.0	5.0
ionic strength	0.03 M	0.06 M	0.06 M	0.30 M	0.32 M
acetic acid	—	—	—	144 mM	144 mM
lecithin	—	—	0.02 mM	—	3.75 mM
Na-taurocholate	—	—	0.08 mM	—	15 mM
NaCl	—	34.2 mM	34.2 mM	203 mM	203 mM
HCl	25.1 mM	25.1 mM	25.1 mM	—	—
NaOH	—	—	—	101.0 mM	101.0 mM

[a]FaSSGF: fasted-state simulated gastric fluid, FeSSIF: fed-state simulated intestinal fluid, $FaSSGF_{blk}$: blank FaSSGF, $FeSSIF_{blk}$: blank FeSSIF.

of some compounds could shift when dissolved in biorelevant media.[15]

Biorelevant media simulate gastric or intestinal fluid in a fed or fasted state by containing various additives.[16,17] The most important with respect to drug dissolution are the surfactants (i.e., lecithin and sodium taurocholate). These amphiphilic molecules arrange themselves onto the solid−liquid interface and modify the wetting behavior by reduction of the contact angle between the drug and the liquid. Moreover, if the critical micellar concentration is exceeded, the drug molecules can become incorporated inside the self-assembled surfactant structures (micelles).[18] Finally, in addition to the solubility, surfactants can also affect the polymorphic changes of a dissolving compound, as shown by Lehto and co-workers.[19]

The aim of the present study was to investigate the solubility of polymorphs of indomethacin, a BCS class II drug, in biorelevant media. Solubility measurements were conducted utilizing the newly developed image-based single-particle-analysis (SPA) method.[20] The method combines optics with fluidics and enables measurement of solubility with less than 0.1 mg of a compound on the basis of the dissolution rate. With the SPA method, the impact of the dissolution media and the effect of the solid-state form on solubility were studied. Moreover, an estimation of the free-energy difference between the two polymorphic forms was made.

MATERIALS AND METHODS

Materials. Indomethacin (γ form) was acquired from Orion Pharma (Espoo, Finland). Hydrochloric acid (98%), acetic acid (≥99.85%), phosphorus pentoxide, and sodium chloride were acquired from Sigma-Aldrich (St. Louis, MO). FaSSIF/FeSSIF/FaSSGF biorelevant powder was acquired from Biorelevant (London, U.K.).

Preparation of α and γ Forms. The γ form of indomethacin was used without further purification or processing. The α form of indomethacin was prepared by dissolving γ indomethacin powder in a 50% (v/v) EtOH/Milli-Q water mixture, followed by slow evaporation of the solvent, which is a modification of the method used by Kaneniwa et al.[21] The obtained crystals were collected and stored over phosphorus pentoxide at ambient temperature.

Dissolution Media. Three kinds of media of pH 1.6 (i.e., HCl; fasted-state simulated gastric fluid, FaSSGF; and blank FaSSGF, $FaSSGF_{blk}$) were prepared according to the instructions of the manufacturer (Biorelevant, London, U.K.). Furthermore, two kinds of media of pH 5.0 were prepared: fed-state simulated intestinal fluid (FeSSIF) and blank FeSSIF ($FeSSIF_{blk}$). FaSSGF and FeSSIF biorelevant media were selected to represent a physiological environment with surfactant molecules present below and above the critical micellar concentration, respectively. The detailed compositions of the media are listed in Table 1.

Image-Based Solubility Measurements. Dissolution experiments utilizing the SPA method were performed using a custom-made flow-through setup (Figure 1). The experiments were conducted at room temperature (22 °C) rather than at 37 °C in order to ensure controlled experimental conditions. The setup enables the trapping of particles under constant-flow conditions. In this way, dissolved molecules are continuously extracted from the chamber, and sink conditions are maintained. As the measurement can be started as soon as the solvent comes in contact with the entrapped particles, the actual solubility of a metastable form can be measured before any possible solid-state transformation occurs that could affect the solubility.

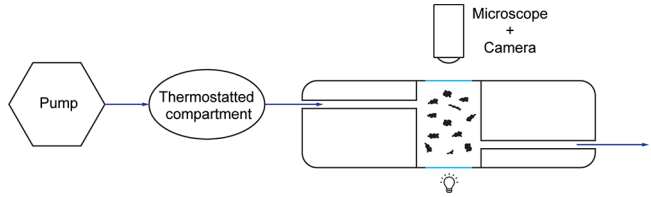

Figure 1. Scheme of the flow-through device (not to scale). Blue arrows present the flow of the solvent. Particles of the compound being analyzed are immobilized in the flow-through chamber. Light access is enabled through the window on the bottom, and imaging of the particles is enabled through the glass window on the top.

In eq 1, at sink conditions, bulk concentration (C_b) can be disregarded because it is practically zero. This means the dissolution rate (dm/dt) is dependent only on the equilibrium solubility at the interface (C_S); k is the setup-dependent transport-rate constant determined as described by Svanbäck.[20]

$$\frac{dm}{dt} = -k(C_S - C_b) \rightarrow \frac{dm}{dt} = -k(C_S) \quad (1)$$

For a single measurement, approximately 10 mL of dissolution medium and less than 0.1 mg of sample were used. Online images were acquired over 15 min through the transparent part of the flow-through chamber using a USB microscope (Gigastone S1-100, Irvine, CA). At least five particles per solid-state form per medium were measured. For the analysis of the image data, a MatLab script was previously developed by Svanbäck and co-workers.[20,22] The script enables quantification of the particle's morphology change (i.e., dissolution rate) and, consequently, calculation of the solubility according to eq 1.

Shake-Flask Solubility Measurements. The solubilities of α and γ indomethacin were measured by the conventional

DOI: 10.1021/acs.analchem.8b05290
Anal. Chem. 2019, 91, 3997−4003

shake-flask method in HCl (pH 1.6), $FaSSGF_{blk}$, and $FeSSIF_{blk}$. A detailed description of the methodology can be found in the Supporting Information on page S-2.

X-ray-Powder Diffraction (XRPD). XRPD diffractograms were recorded using an Empyrean diffractometer (Malvern Panalytical B.V., Almelo, The Netherlands) with Cu Kα radiation (λ = 1.54 Å) and a divergence slit of 1/8°. Samples were packed into the aluminum holder and measured at 45 kV and 40 mA from 5 to 35° (2θ) with a step size of 0.0066°.

Differential-Scanning Calorimetry (DSC). DSC experiments were performed using a DSC823e (Mettler-Toledo, Greifensee, Switzerland) equipped with a refrigerated cooling system (Julabo FT 900, Seelbach, Germany). Nitrogen was used as a purge gas (50 mL/min).

Samples (2−5 mg) were tightly packed into standard aluminum crucibles (40 μL) with pierced lids. Two different procedures were used in these measurements. For determination of melting temperature and enthalpy, the samples were equilibrated at 25 °C for 3 min and then linearly heated with a heating rate of 10 °C/min to 180 °C. For determination of heat capacities, the samples were equilibrated at 140 °C and then heated up to 180 °C using a TOPEM-modulated heating program with a heating rate of 1 °C/min and a pulse height of 1 °C. Samples were measured in triplicate, and thermal events were analyzed using STARe software (Mettler-Toledo, Greifensee, Switzerland). Temperatures of melting, enthalpies of melting, and heat capacities were used to estimate the free-energy difference between the α and γ polymorphs.

Fourier-Transform Infrared (FT-IR) and Time-Resolved Raman Spectroscopy. FT-IR measurements were conducted using a Burker Vertex 70 spectrometer (Burker Optik, Ettlingen, Germany). The spectrometer was coupled with an attenuated-total-reflectance (ATR) accessory, a single-reflection diamond crystal (MIRacle, Pike Technologies, Madison, WI). The final spectrum was the mean of 128 scans with a resolution of 2 cm^{-1} and a spectral range from 650 to 4000 cm^{-1}. The absorbance spectra were obtained using OPUS software (v. 5.0, Burker Optik, Ettlingen, Germany).

The time-resolved Raman measurements were performed using a TG532 M1 Raman Spectrometer System (TimeGate Instruments, Oulu, Finland). The average power used was 60 mW, the pulse width was 150 ps, the spot size was 85 μm, and the repetition rate was 40 kHz. Samples were packed in an aluminum holder and measured. During the measurements, the focal point was moved continuously using a SampleCube provided by TimeGate Instruments (Oulu, Finland). The spectral range was recorded at 11 consecutive detector positions from 900 to 1800 cm^{-1}. The data was processed using a MatLab-based program provided by TimeGate Instruments (Oulu, Finland).

Scanning Electron Microscopy. Samples were placed on a sample holder using double-sided carbon adhesive tape. Upon adhesion, samples were coated with platinum in a high-vacuum evaporator (Q150TS, Quorum Technologies, Lewes, U.K.) and imaged with a Quanta 250 FEG SEM (FEI Company, Hillsboro, OR). Images were taken with 500× magnification.

RESULTS AND DISCUSSION

Characterization of the Solid-State Forms. Results of the solid-state characterization are presented in Figure 2 and summarized in Table 2. Spectroscopic and thermal analyses of the samples were in good agreement with previously reported

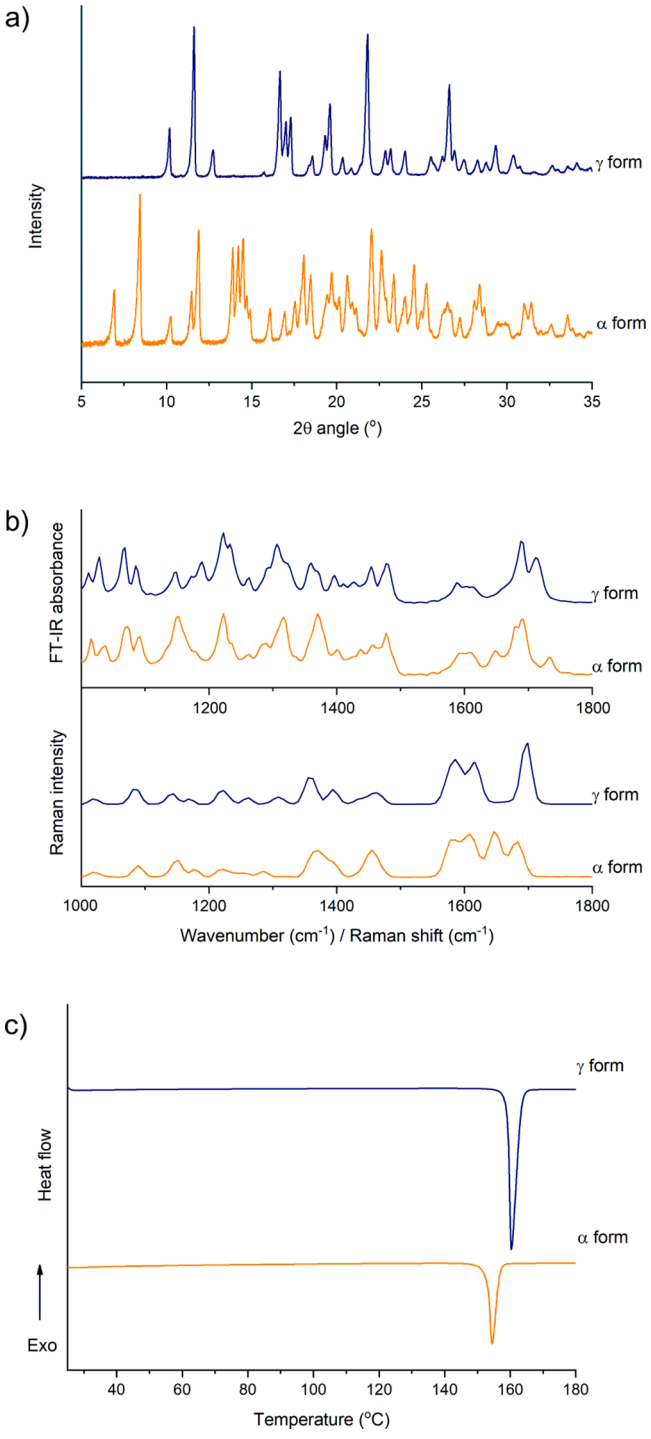

Figure 2. XRPD diffractograms (a), FT-IR and Raman spectra (b), and DSC thermograms (c) of the α and γ solid-state forms of indomethacin.

data on the thermodynamically metastable α and stable γ solid-state forms of indomethacin.[23−26] Moreover, experimental XRPD diffractograms of the α and γ forms coincide with those reported in the Cambridge Structural Database (INDMET02 and INDMET01, respectively).

The benzoyl-stretching mode, listed in Table 2, represents the difference in H-bonding in the α and γ crystals. The two stretching modes of the C═O groups, H-bonded and non-H-bonded, are present in α crystals, and only one stretching mode, non-H-bonded, is present in γ crystals.[26] The difference

DOI: 10.1021/acs.analchem.8b05290
Anal. Chem. 2019, 91, 3997−4003

Table 2. Unique XRPD Peaks, Benzoyl-C=O-Stretching-Mode Vibrations, and Thermal Properties of the α and γ Indomethacin Solid-State Forms[a]

	XRPD	C=O-stretching mode (cm^{-1})		DSC			
solid-state form	unique peak positions (°, 2θ)	FT-IR	Raman	T_m (°C)	ΔH_m (J/g)	C_p (J/(g K))	$C_{p,L}$ (J/(g K))
α form	6.9, 8.4, 14.2	1680, 1649	1684, 1646	152.8 ± 0.1	97.5 ± 2.6	2.3 ± 0.4	2.0 ± 0.4
γ form	12.7, 16.7, 21.8	1690	1699	159.1 ± 0.1	106.3 ± 1.5	1.7 ± 0.2	2.1 ± 0.1

[a]T_m: melting point, ΔH_m: melting enthalpy, C_p: heat capacity, $C_{p,L}$: heat capacity upon melting.

in H-bonding is associated with different orientations of the molecules in the crystalline lattice. This difference on the molecular scale is translated to the macroscopically distinct shapes of α and γ crystals. In Figure 3, needle-shaped α crystals can be clearly distinguished from prismatic γ crystals.

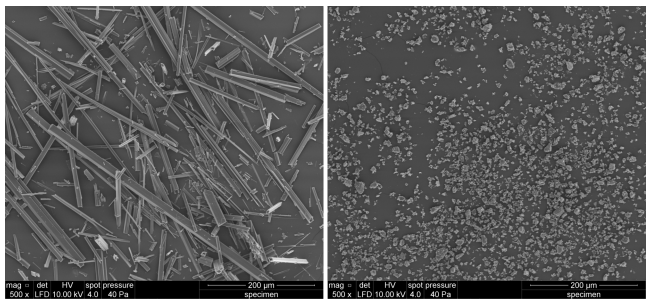

Figure 3. SEM image of the α (left) and γ (right) solid-state forms of indomethacin.

SPA-Method Solubility Measurements: Impact of the Solid-State Form. Using the image-based SPA method, the solubilities of the α and γ solid-state forms of indomethacin in selected media were measured (Figure 4). In the time span of

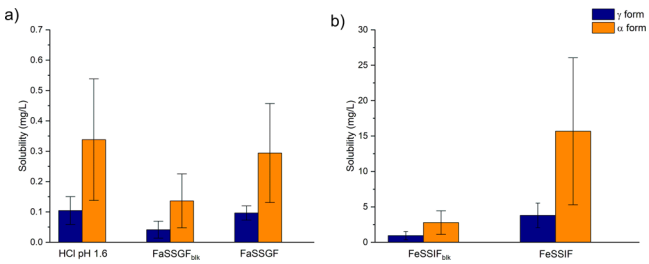

Figure 4. Solubility of indomethacin α and γ solid-state forms in media with pH 1.6 (a) and media with pH 5.0 (b) as measured with the SPA method. The effects of pH and surfactants (FaSSGF and FeSSIF) on solubility can be noted. FaSSGF: fasted-state simulated gastric fluid, FeSSIF: fed-state simulated intestinal fluid, FaSSGF$_{blk}$: blank FaSSGF, FeSSIF$_{blk}$: blank FeSSIF.

the measurements, there were constant increases in dissolved mass for both solid-state forms. Hence, it was concluded that no solid-state change took place that would affect the solubility of the dissolving form. Moreover, no effect of particle morphology on the SPA solubility values was found (Supplementary Figures S1 and S2). Therefore, the apparent equilibrium solubility of the α form and the thermodynamic-equilibrium solubility of the γ form were measured. Additionally, the solubilities of α and γ indomethacin were also measured by the conventional shake-flask method (Supplementary Table S1 and Figures S3 and S4).

The ratio of α- to γ-solid-state-form solubility was constant at 3.3 ± 0.5 in all of the studied media. The observed ratio was higher than the value of 1.7 ± 0.4 obtained by the shake-flask experiment in this study (Supporting Information, page S-2). Moreover, the ratio was also higher than the 1.1 value obtained by Hancock et al., where the α- to γ-solubility ratio was measured in 200 mL of deionized water at 45 °C using a flat-bottomed, water-jacketed, glass vessel with a propeller stirrer.[9] Their samples were withdrawn at regular intervals through a 0.22 μm filter and diluted with a standard solution of indomethacin in 50:50 methanol/water, and the concentration was measured by UV−visible spectrometry. Both procedures, the shake-flask experiment conducted in this study and the one performed by Hancock et al., have several more steps when compared with the straightforward SPA method. Nevertheless, Hancock et al. also found that the reported solubility ratio of crystalline polymorphs varies between 1.1 and 4.0, which is in agreement with the α- to γ-solubility ratio observed in this study.

The constant solubility ratio in HCl, FaSSGF$_{blk}$, FaSSGF, FeSSIF$_{blk}$, and FeSSIF media indicates that changes in the ionic strength, pH, or surfactant concentration of the medium affect the solubility of both indomethacin crystalline solid-state forms to the same extent.

SPA-Method Solubility Measurements: Impact of the Dissolution Media. To evaluate the impact of the dissolution media, ratios of the average solubility values (R_S) of the same indomethacin solid-state form measured in different media were calculated (eq 2). S_x and S_y are the average solubility values in media x and y. It must be noted that the standard deviation of the calculated ratios is relatively large and most likely results from the particulate nature of the SPA measurement, discussed in more detail in the Particle Statistics section.

$$R_S = \frac{S_x}{S_y} \quad (2)$$

The composition of the dissolution media affects the solubility of indomethacin. At pH 1.6, an increase in the ionic strength of the dissolution medium (from HCl to FaSSGF$_{blk}$) resulted in decreases in the solubilities of both solid-state forms (Table 3). On the other hand, the addition of surfactants (from FaSSGF$_{blk}$ to FaSSGF) resulted in 2.1 and

Table 3. Ratios of Average Solubility Values Obtained with the Image-Based SPA Method for the Same Solid-State Form Measured in Different Solvents

solubility ratio (R_S)	α form	γ form
FaSSGF$_{blk}$/HCl	0.4	0.4
FaSSGF/HCl	0.9	1.0
FaSSGF/FaSSGF$_{blk}$	2.1	2.5
FeSSIF/FeSSIF$_{blk}$	5.6	4.0

[a]SPA: single-particle analysis, HCl: HCl pH 1.6, FaSSGF$_{blk}$: blank FaSSGF, FeSSIF$_{blk}$: blank FeSSIF.

DOI: 10.1021/acs.analchem.8b05290
Anal. Chem. 2019, 91, 3997−4003

2.5 times higher solubilities of the α and γ forms. Consequently, increases in both the ionic strength of the dissolution medium and the surfactant concentration (from HCl to FaSSGF) cancel each other out and do not have a significant impact on solubility.

In FeSSIF, the concentrations of sodium taurocholate and lecithin were above their respective critical micellar concentrations (CMC).[27,28] Therefore, surfactant molecules were arranged in micelles, spherical structures in which the hydrophilic regions (heads) are in contact with the solvent, and the hydrophobic regions (chains) are contained within the micelle center. In FaSSGF, the concentrations of sodium taurocholate and lecithin are below the CMC. Thus, micelles were not formed. The occurrence of micelles in dissolution media (from $FeSSIF_{blk}$ to FeSSIF) resulted in 5.6- and 4.0-fold increases of the α- and γ-form solubilities, respectively. A similar increase (7.3-fold) in the solubility of the γ form at 37 °C using a μDISS profiler was also measured by Fagerberg and co-workers.[15] From a physicochemical perspective, the solubility was increased because of the two following phenomena: lowering of the solvent's surface tension (in both FeSSIF and FaSSGF) and distribution of hydrophobic indomethacin molecules inside the micelles (only in FeSSIF).

Particle Statistics. Because of the large relative standard deviations (RSD) of the collected data (55 ± 15%), the Mann−Whitney test was used to determine if the measured particles of the α and γ forms belong to two separate populations. The results (Table 4) show that there is a significant difference in the solubility values of the α and γ forms in all of the five media used. Therefore, despite the relatively large RSDs between the solubilities of individual particles measured with the image-based SPA method, the samples were still distinct enough to show that they belong to different populations and therefore different solid-state forms of indomethacin.

Table 4. Solubility Values of the α and γ Forms of Indomethacin in Different Media and Results of Multiple Mann−Whitney Tests

	solubility (mg/L)		*p*-value
solvent	α form	γ form	α vs γ
HCl	0.34 ± 0.20	0.10 ± 0.05	0.001
$FaSSGF_{blk}$	0.14 ± 0.09	0.04 ± 0.03	0.001
FaSSGF	0.29 ± 0.16	0.10 ± 0.02	0.026
$FeSSIF_{blk}$	2.79 ± 1.67	0.94 ± 0.58	0.001
FeSSIF	15.7 ± 10.4	3.80 ± 1.74	0.009

[a]HCl: HCl pH 1.6, $FaSSGF_{blk}$: blank FaSSGF, $FeSSIF_{blk}$: blank FeSSIF, *p*-value: significance level (significant at $p < 0.05$).

One of the reasons for the high RSD values can be the SPA method itself, which is still in the development process. With further improvements in the experimental setup, control of experimental conditions, and image quality, the RSD may be reduced. Nevertheless, one should consider another aspect of this phenomenon. At its core, the SPA method measures the solubility of individual particles, and the solubility of the compound is the average of the solubility values of all the single particles measured.

In principle, the equilibrium solubility in the shake-flask method is reached after an equilibration period of up to several days, during which a compound is transformed into its most thermodynamically stable form with the lowest solubility.[29] With the image-based SPA method, even the equilibrium solubility of the thermodynamically stable γ solid-state form was approached in a dynamic manner in a matter of minutes, without any equilibration period.

Even if the compound is in its most stable solid-state form, the surface energy of individual particles is not unity, but it most likely follows the Maxwell−Boltzmann distribution.[30] Therefore, a single solid-state form presents a population of particles, of which each has a slightly different surface energy. To our knowledge, this could also contribute to the high variation of the solubility data collected with the SPA method compared with that of the shake-flask method, where this particle-to-particle energy difference is already averaged out by using several milligrams of a compound and thus a multitude of particles.[31] It should also be noted that the uncertainty of solubility values reported in the literature is in the range of 0.6 log units.[32] In contrast, the uncertainty of the SPA measurements was 0.26 log units.

Estimation of the Free-Energy Difference between Polymorphs. The free-energy difference between two polymorphs can be estimated from their melting data or their respective solubility values. For the former, according to Yu et al.,[6] to estimate the difference in enthalpy (ΔH_m) and entropy (ΔS_m) of the melting process, eqs 3 and 4, respectively, can be used under two conditions: (a) the difference between the melting points of the polymorphs is less than 20 K (it is 6.3 K for α and γ indomethacin) and (b) ($C_{p,L} - C_{p,\gamma}$) is assumed to be constant.

$$\Delta H_m = \Delta H_{m,\alpha} - \Delta H_{m,\gamma} + (C_{p,L} - C_{p,\gamma})(T_{m,\gamma} - T_{m,\alpha}) \tag{3}$$

$$\Delta S_m = \frac{\Delta H_{m,\alpha}}{T_{m,\alpha}} - \frac{\Delta H_{m,\gamma}}{T_{m,\gamma}} + (C_{p,L} - C_{p,\gamma})\ln\left(\frac{T_{m,\gamma}}{T_{m,\alpha}}\right) \tag{4}$$

In eqs 3 and 4, $\Delta H_{m,x}$ is the melting-enthalpy change, and $T_{m,x}$ is the melting temperature of the respective polymorphic form. $C_{p,L}$ and $C_{p,\gamma}$ are the heat capacities of the supercooled liquid state and γ form, respectively. By combining eqs 3 and 4 with the well-established relation $\Delta G_0 = \Delta H - T\Delta S$, we obtain eq 5, where ΔG_0 is the free-energy difference at $T_{m,\alpha}$.

$$\Delta G_0 = \Delta H_{m,\gamma}\left(\frac{T_{m,\alpha}}{T_{m,\gamma}} - 1\right) + (C_{p,L} - C_{p,\gamma}) \times \left[T_{m,\gamma} - T_{m,\alpha} - (T_{m,\alpha})\ln\left(\frac{T_{m,\gamma}}{T_{m,\alpha}}\right)\right] \tag{5}$$

To extrapolate the ΔG to room temperature, a correction for nonlinearity has to be made if $(C_{p,\gamma} - C_{p,\alpha}) \neq 0$, as is the case with α and γ indomethacin polymorphs (Table 2). In this place, eq 6, also derived by Yu et al.,[6] can be used, where $(C_{p,\gamma} - C_{p,\alpha})_0$ is the value of $(C_{p,\gamma} - C_{p,\alpha})$ at $T_{m,\alpha}$. A reasonable estimate of this value can be made by subtracting the heat-capacity changes upon melting, $(C_{p,L} - C_{p,\alpha})$ and $(C_{p,L} - C_{p,\gamma})$.

$$\Delta G(T) = \Delta G_0 - \Delta S_0(T - T_{m,\alpha}) - \frac{(C_{p,\gamma} - C_{p,\alpha})_0(T - T_{m,\alpha})^2}{2T_{m,\alpha}} \tag{6}$$

The estimated ΔG between the α and γ polymorphs amounts to 12 ± 7 J/g. The high standard error of the results

DOI: 10.1021/acs.analchem.8b05290
Anal. Chem. 2019, 91, 3997−4003

represents the imprecision of the above free-energy-difference estimation, which originates from an attempt to precisely measure a small energy difference of a process with high energy content: melting.

On the other hand, the ΔG between the polymorphs is directly proportional to their solubilities.[7] Therefore, the estimation of the free-energy difference can also be obtained using eq 7, with R, T, and S_x being the gas constant, the ambient temperature, and the solubilities of the polymorphs, respectively. Inserting the α- to γ-solubility ratio obtained with the SPA method into eq 7, a value of 8 ± 1 J/g is obtained. The result is more precise, and it fits in the range of 12 ± 7 J/g.

$$\Delta G = R \times T \times \ln\left(\frac{S_\alpha}{S_\gamma}\right) \tag{7}$$

The metastable α polymorph has a higher energy content than the stable γ polymorph, and the difference exceeds randomizing thermal energy. The thermal energy (ET) of a system at room temperature is calculated as ET = $R \times T_{22°C}$ = 2.45 kJ/mol. The magnitude of ET can be used as a rough indicator of the interaction strength between molecules.[30] This means that if the interaction energy or, in our case, the difference in free energy, ΔG, exceeds ET, it will overcome the opposing disorganizing effect of thermal motion. The calculated ΔG from the solubility ratios of the α and γ polymorphs expressed in molar units amounts to 2.9 kJ/mol, whereas the shake-flask solubility ratios give a value of 1.3 kJ/mol. It is well-known that the α form of indomethacin is stable at room temperature, which would substantiate the result obtained by the theoretical estimation based on DSC measurements and the SPA method.

CONCLUSIONS

In this study, the SPA method was proven capable of determining the solubility of two different solid-state forms of the same drug compound. The solubility ratio of the α to γ solid-state forms of indomethacin is constant at 3.3 ± 0.5 and is not affected by pH, ionic-strength, or surfactant-concentration changes below or above CMC. Therefore, the only factor affecting the solubility ratio is the ΔG (2.9 kJ/mol) between the two polymorphs.

The use of biorelevant media resulted in significantly higher solubility values when compared with the respective values in aqueous blank media. This indicates that for a solubility study aiming to estimate solubility, bioavailability, or BCS classification, biorelevant dissolution media should be used over blank aqueous buffers.

Finally, the SPA method can be characterized as a quick-turnover and low-solvent- and low-substance-consumption method, thus making it a highly appealing research tool when it comes to polymorph-solubility screening.

ASSOCIATED CONTENT

Supporting Information

The Supporting Information is available free of charge on the ACS Publications website at DOI: 10.1021/acs.analchem.8b05290.

Particle morphology, shake-flask solubility measurements, solubility values obtained for α and γ indomethacin by the conventional shake-flask method and the SPA method, solubility of individual particles plotted vs particle-shape descriptors for α and γ indomethacin, XRPD diffractograms and DSC thermograms of the remaining solid after 72 h of a shake-flask experiment started with pure α form of indomethacin (PDF)

AUTHOR INFORMATION

Corresponding Author

*E-mail: jernej.stukelj@helsinki.fi.

ORCID

Jernej Štukelj: 0000-0002-1452-4310

Clare J. Strachan: 0000-0003-3134-8918

Author Contributions

J.S., S.S., J.K, C.J.S., and J.Y. conceived the project and designed the experiments. J.S. performed the experiments and wrote the manuscript. S.S., J.K., C.J.S., and J.Y. reviewed the manuscript.

Notes

The authors declare the following competing financial interest(s): J.S., S.S., and J.Y. are shareholders of The Solubility Company Oy, which owns the intellectual property rights to the SPA method.

ACKNOWLEDGMENTS

J.S., S.S., and J.Y. acknowledge TEKES (grant no. 4511/31/2016). J.S. and C.J.S. acknowledge the Academy of Finland (grant no. 289398). J.S. acknowledges the Doctoral Programme in Drug Research (DPDR) for funding. J.S. acknowledges Alyce Whipp for help with language editing of the manuscript.

REFERENCES

(1) Lipinski, C. A. *Am. Pharm. Rev.* **2009**, *3*, 38−40.

(2) Huang, L. F.; Tong, W. Q. *Adv. Drug Delivery Rev.* **2004**, *56*, 321−334.

(3) Lipinski, C. A. *J. Pharmacol. Toxicol. Methods* **2000**, *44*, 235−249.

(4) Gardner, C. R.; Walsh, C. T.; Almarsson, O. *Nat. Rev. Drug Discovery* **2004**, *3*, 926−934.

(5) Chemburkar, S. R.; Bauer, J.; Deming, K.; Spiwek, H.; Patel, K.; Morris, J.; Henry, R.; Spanton, S.; Dziki, W.; Porter, W.; Quick, J.; Bauer, P.; Donaubauer, J.; Narayanan, B. A.; Soldani, M.; Riley, D.; McFarland, K. *Org. Process Res. Dev.* **2000**, *4*, 413−417.

(6) Yu, L. *J. Pharm. Sci.* **1995**, *84*, 966−974.

(7) Augustijns, P.; Brewster, M. E. Solvent Systems and Their Selection in Pharmaceutics and Biopharmaceutics. In *Biotechnology: Pharmaceutical Aspects*; Borchardt, R. T., Diddaugh, C. R., Eds.; Springer: New York, 2007; Vol. *VI*, pp 53−60.

(8) Bhattachar, S. N.; Deschenes, L. A.; Wesley, J. A. *Drug Discovery Today* **2006**, *11*, 1012−1018.

(9) Hancock, B. C.; Parks, M. *Pharm. Res.* **2000**, *17*, 397−404.

(10) Florence, A. T.; Attwood, D. The Solubility of Drugs. In *Physicochemical Principles of Pharmacy*, 4th ed.; Pharmaceutical Press: London, 2006; pp 139−176.

(11) Yalkowsky, S. H.; Valvani, S. C. *J. Pharm. Sci.* **1980**, *69*, 912−922.

(12) Pudipeddi, M.; Serajuddin, A. T. M. *J. Pharm. Sci.* **2005**, *94*, 929−939.

(13) Amidon, G. L.; Lennernäs, H.; Shah, V. P.; Crison, J. R. *Pharm. Res.* **1995**, *12*, 413−420.

(14) Shah, V. P.; Amidon, G. L. *AAPS J.* **2014**, *16*, 894−898.

(15) Fagerberg, J. H.; Tsinman, O.; Sun, Na; Tsinman, K.; Avdeef, A.; Bergström, C. A. S. *Mol. Pharmaceutics* **2010**, *7*, 1419−1430.

(16) Klein, S. *AAPS J.* **2010**, *12*, 397−406.

DOI: 10.1021/acs.analchem.8b05290
Anal. Chem. 2019, 91, 3997−4003

(17) Jantratid, E.; Janssen, N.; Reppas, C.; Dressman, J. B. *Pharm. Res.* **2008**, *25*, 1663−1676.
(18) Vinarov, Z.; Katev, V.; Radeva, D.; Tcholakova, S.; Denkov, N. D. *Drug Dev. Ind. Pharm.* **2018**, *44*, 677−686.
(19) Lehto, P.; Aaltonen, J.; Tenho, M.; Rantanen, J.; Hirvonen, J.; Tanninen, V. P.; Peltonen, L. *J. Pharm. Sci.* **2009**, *98*, 985−996.
(20) Svanbäck, S. *Toward accurate high-throughput physicochemical profiling using image-based single-particle analysis*. Ph.D. Dissertation, University of Helsinki, Helsinki, Finland, 2016.
(21) Kaneniwa, N.; Otsuka, M.; Hayashi, T. *Chem. Pharm. Bull.* **1985**, *33*, 3447−3455.
(22) Svanbäck, S.; Ehlers, H.; Antikainen, O.; Yliruusi, J. *Anal. Chem.* **2015**, *87*, 5041−5045.
(23) Savolainen, M.; Heinz, A.; Strachan, C. J.; Gordon, K. C.; Yliruusi, J.; Rades, T.; Sandler, N. *Eur. J. Pharm. Sci.* **2007**, *30*, 113−123.
(24) Heinz, A.; Savolainen, M.; Rades, T.; Strachan, C. J. *Eur. J. Pharm. Sci.* **2007**, *32*, 182−192.
(25) Borka, L. *Acta Pharm. Suec.* **1974**, *11*, 295−303.
(26) Surwase, S. A.; Boetker, J. P.; Saville, D.; Boyd, B. J.; Gordon, K. C.; Peltonen, L.; Strachan, C. J. *Mol. Pharmaceutics* **2013**, *10*, 4472−4480.
(27) Kratohvil, J. P.; Hsu, W. P.; Jacobs, M. A.; Aminabhavi, T. M.; Mukunoki, Y. *Colloid Polym. Sci.* **1983**, *261*, 781−785.
(28) Martínez-Landeira, P.; Ruso, J. M.; Prieto, G.; Sarmiento, F. *J. Chem. Eng. Data* **2002**, *47*, 1017−1021.
(29) Sugano, K.; Okazaki, A.; Sugimoto, S.; Tavornvipas, S.; Omura, A.; Mano, T. *Drug Metab. Pharmacokinet.* **2007**, *22*, 225−254.
(30) Israelachvili, J. N. Thermodynamic and Statistical Aspects of Intermolecular Forces. In *Intermolecular and Surface Forces*, 3rd ed.; Israelachvili, J. N., Ed.; Elsevier: Oxford, 2011; pp 23−51.
(31) Baka, E.; Comer, J. E. A.; Takács-Novák, K. *J. Pharm. Biomed. Anal.* **2008**, *46*, 335−341.
(32) Jorgensen, W. L.; Duffy, E. M. *Adv. Drug Delivery Rev.* **2002**, *54*, 355−366.

DOI: 10.1021/acs.analchem.8b05290
Anal. Chem. 2019, 91, 3997−4003